Terra Nova

doi: 10.1111/j.1365-3121.2011.01006.x

Emplacement and exhumation of the Kuznetsk-Alatau basement (Siberia): implications for the tectonic evolution of the Central Asian Orogenic Belt and sediment supply to the Kuznetsk, Minusa and West Siberian Basins

Johan De Grave,[1] Stijn Glorie,[1] Fedor I. Zhimulev,[2] Mikhail M. Buslov,[2] Marlina Elburg,[1] Frank Vanhaecke[3] and Peter Van den haute[1]

[1]*Department of Mineralogy & Petrology, Ghent University, Ghent, Belgium;* [2]*Institute of Geology & Mineralogy, Siberian Branch, Russian Academy of Sciences, Novosibirsk, Russia;* [3]*Department of Analytical Chemistry, Ghent University, Ghent, Belgium*

ABSTRACT

New geochronological data [zircon U/Pb, titanite fission-track (TFT) and apatite fission-track (AFT) dating and apatite (U-Th-Sm)/He thermochronology] and thermal history modelling yield constraints on the development of the granitoid basement of the Kuznetsk-Alatau Mountains, southern Siberia. The final stages of magmatism in the Kuznetsk-Alatau palaeo-island-arc are Late Cambrian, and collision of the arc with Siberia occurred in the Early Ordovician. The basement was exhumed by the Early Devonian. Continuous Devonian–Early Triassic sedimentation filled the adjoining Kuznetsk and Minusa basins and buried (and re-heated) the Kuznetsk-Alatau basement. After initial Pangaea break-up and Siberian flood-basalt magmatism, the basement reached TFT and AFT retention-temperatures in the Middle Triassic and Early Cretaceous, respectively, during denudation-induced cooling.

Terra Nova, 23, 248–256, 2011

Introduction and geological setting

The Altai–Sayan fold belt forms part of the intracontinental Central Asian Orogenic Belt (CAOB; Fig. 1), which was partially reactivated as a far field effect of India-Eurasia convergence (De Grave *et al*., 2007). The basement of the CAOB, and of Altai–Sayan in particular, is mainly composed of Late Precambrian and Palaeozoic tectonic units. These units – micro-continents, island-arcs, accretionary complexes and seamounts – often demarcated by ophiolite complexes, assembled into the proto-Asian continent during Palaeozoic collision–accretion events (Windley *et al*., 2007) and evolution of the Palaeo-Asian Ocean (PAO) (Khain *et al*., 2003; Dobretsov and Buslov, 2007; Buslov, 2011). Voluminous granitoid intrusions are associated with these accretion–collision events. Many parts of the CAOB (or Altaids; Şengör *et al*., 1993), including Altai–Sayan, were subjected to Late Palaeozoic strike-slip deformation (Buslov *et al*., 2003) and Mesozoic reactivation that exhumed the crystalline basement (De Grave *et al*., 2009) and filled major Mesozoic basins (Davies *et al*., 2010). The Late Palaeozoic and Mesozoic basins surrounding the Kuznetsk-Alatau area (Minusa, Kuznetsk and West Siberian Basin) have attracted attention in relation to their important hydrocarbon potential and their association with the *c*. 250 Ma Siberian flood basalts. The adjoining basement blocks hold key information on the timing of sedimentary input and regional thermal history.

The Kuznetsk-Alatau in fact represents the northernmost section of the Altai–Sayan basement (Fig. 1). Although Cenozoic tectonic reactivation produced a significant modern Altai–Sayan mountain belt to the south, the Kuznetsk-Alatau region shows only embryonic signs of recent deformation (Allen and Davies, 2007; Novikov *et al*., 2008) and is characterized by a low, hilly landscape. Absolute age constraints on its Palaeozoic basement, Meso-Cenozoic evolution and topography are limited. This study, centred on multi-method chronology and supported by detailed mapping, was therefore undertaken.

Correspondence: Johan De Grave, Department of Mineralogy & Petrology, Ghent University, Krijgslaan 281/S8, WE13, B-9000 Gent, Belgium. Tel.: +32 9264 4564; fax: +32 9264 4984; e-mail: johan.degrave@ugent.be

Kuznetsk-Alatau island-arc

The Palaeozoic basement of the Kuznetsk-Alatau forms a ridge between the Late Palaeozoic–Mesozoic Minusa (east) and Kuznetsk Basin (west) (Figs 1 and 2). The Kuznetsk-Alatau terrane can be subdivided into four structural blocks: the Zolotokitat, Martaiga, Iuys-Batenev and Mras-Su blocks (Fig. 2; Kazansky *et al*., 2003). Our study focuses on the crystalline basement of the Iuys-Batenev block. The basement of these blocks constitutes the Ediacaran–Cambrian Kuznetsk-Alatau palaeo-island-arc, and is mainly composed of volcanic rocks with a sandstone and limestone cover and are extensively intruded by Cambrian–Ordovician granitoids (Figs 2 and 3). Kuznetsk-Alatau forms part of a more extensive island-arc system, stretching into the Gorny-Altai terrane to the south (Buslov *et al*., 2002; Dobretsov and Buslov, 2007). Presently, these basement rocks form a complex sequence of imbricated, overthrusted nappes. In the Early Ordovician, the Kuznetsk-Alatau island-arc accreted to Siberia due to progressive closure of the PAO. The collision is accompanied by deposition of Ordovician molasse and emplacement of subalkaline intrusions.

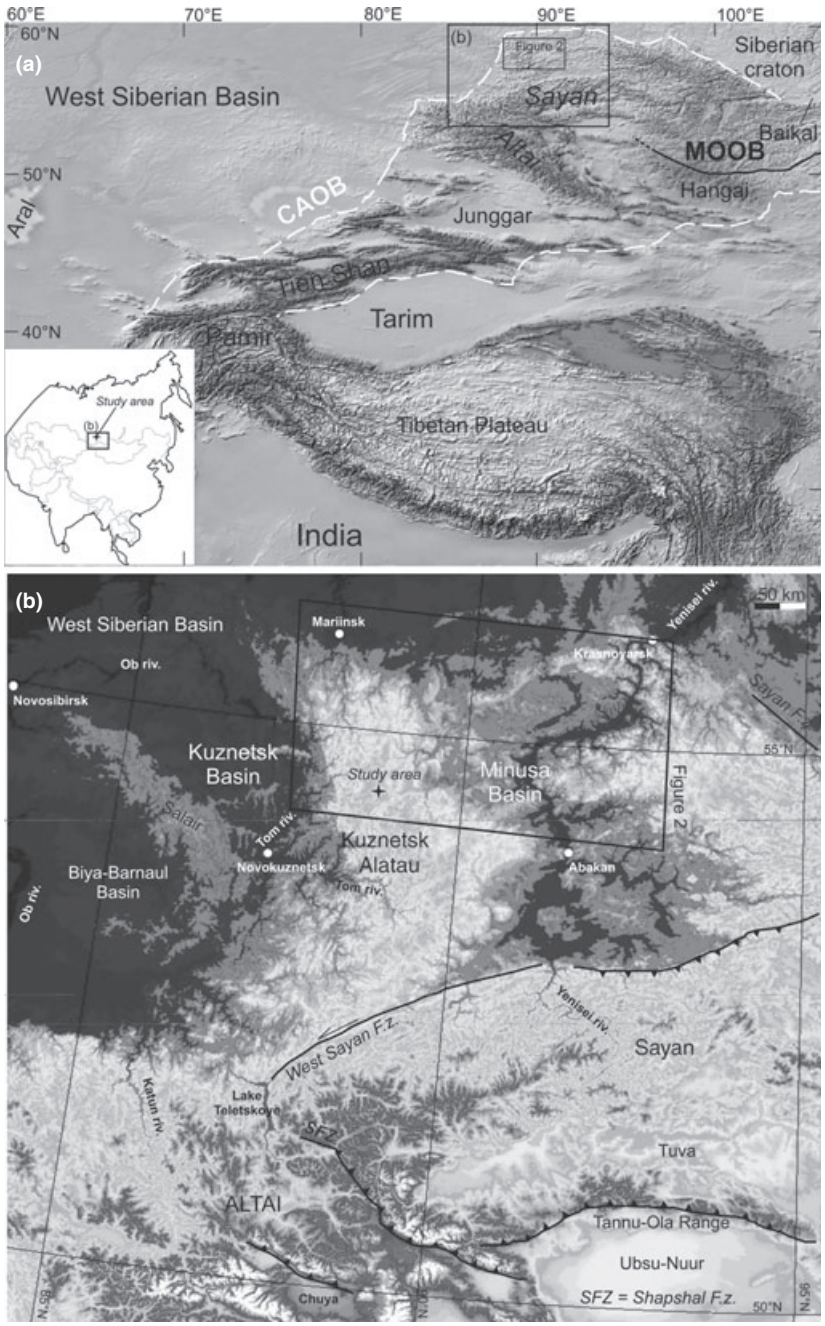

Fig. 1 General location of the study area in Southern Siberia: (a) Kuznetsk-Alatau forms the northern part of the Altai–Sayan fold-belt in the Central Asian Orogenic Belt (CAOB). The Mongol–Okhotsk Orogenic Belt (MOOB) is located to the south (east) of this area. (b) Kuznetsk-Alatau is a Palaeo-Mesozoic fold belt that separates the Kuznetsk Basin (west) and the Minusa Basin (east). It is further delimited by the West Siberian Basin (north) and the present-day Altai–Sayan orogen (south). The study area is located in the northern section of Kuznetsk-Alatau.

Minusa Basin

The Minusa Basin, east of the Kuznetsk-Alatau ridge (Fig. 2), formed in the Early Devonian on Siberia's Palaeozoic margin and evolved into a back-arc basin, behind the developing Siberian active margin later in the Devonian. Devonian–Carboniferous sediments dominate the basin (Fedoseev, 2008). A basal Early Devonian erosional conglomerate lies on the Kuznetsk-Alatau basement along a sharp angular unconformity (Fig. 3b). It is followed by an Early Devonian volcanic unit (Byskar Series) with alkaline basalts, andesites, rhyolites and tuffs. This unit is covered by a continuous Middle Devonian–Early Permian sequence of sandstones with conglomerate lenses, limestones and mudstones. At the base, they reflect shallow marine conditions with a regressive transition to continental conditions up-section (including coal seams, Sekretarev and Lipishanov, 2000).

An unconformity marks the boundary with overlying Late Permian–Early Triassic sediments. Widespread, but isolated pockets of coal-bearing Jurassic sediments occur above a Late Triassic–Early Jurassic unconformity. These are in turn cut by a Late Jurassic–Early Cretaceous unconformity and overlying Cretaceous–Early Cenozoic sediments.

Kuznetsk Basin

West of Kuznetsk-Alatau lies the Kuznetsk Basin, situated at the southern edge of the vast, hydrocarbon-rich West Siberian Basin (Vyssotski *et al.*, 2006) (Fig 1). Its sediments are predominantly Permian–Cretaceous (Buslov *et al.*, 2010; Davies *et al.*, 2010). A basal Late Carboniferous–Early Permian unit of non-marine sediments is followed by the main (continuous) Permian–Middle Triassic continental succession, rich in coal and containing basalt units of *c.* 250 Ma (Reichow *et al.*, 2009; Buslov *et al.*, 2010). These are related to the Siberian flood basalts that form the world's most extensive continental Large Igneous Province (LIP). The Permian–Triassic deposits show signs of post-Middle Triassic compressional deformation (Davies *et al.*, 2010).

Early–Middle Jurassic sediments (~1 km) cover the Permian–Middle Triassic units unconformably and are coal-bearing. Another unconformity separates these strata from Early Cretaceous sediments that represent the terminal basin infill. In contrast to all other sediments, the Cretaceous is considered marine in nature. The Mesozoic sediments are folded, suggesting post-Early Cretaceous deformation (Davies *et al.*, 2010).

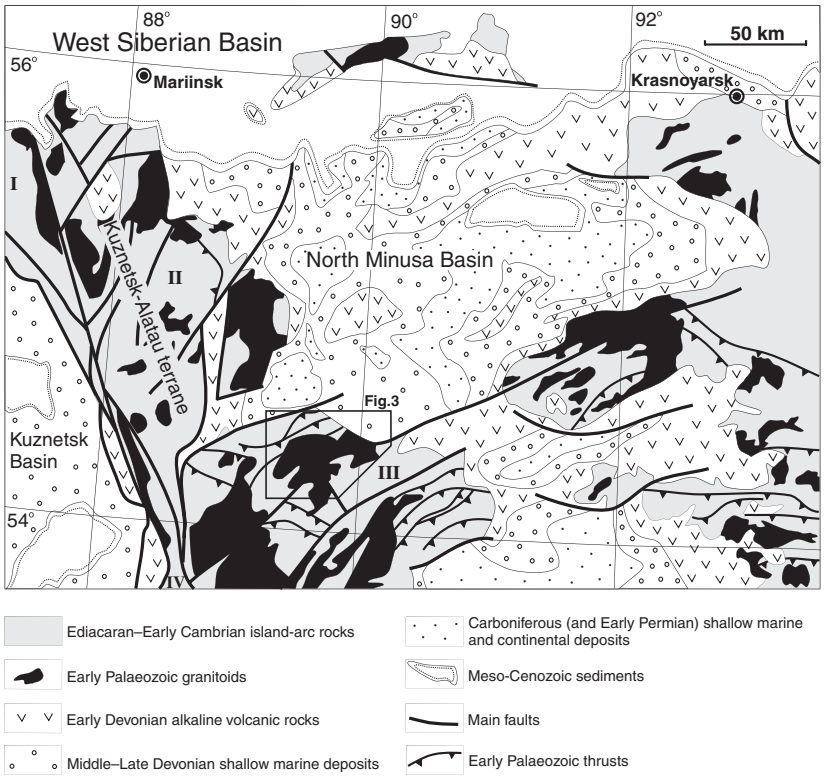

Fig. 2 Schematic geological map of the Kuznetsk-Alatau area and adjoining basins. Tectonic blocks composing Kuznetsk-Alatau: I = Zolotokitat block, II = Martaiga block, III = Iuys-Batenev block, IV = Mras-Su block.

The Early Jurassic is characterized by conglomerates with large clasts, indicating a high energy depositional environment. Near-identical observations on sediment fill, type, distribution, provenance and unconformities were made for the southeastern edge of the West Siberian Basin, near Mariinsk–Krasnoyarsk (Le Heron *et al.*, 2008) at the Minusa Basin transition (Figs 1 and 2).

Samples and methodology

Five samples from the granitoid basement of the Iuys-Batenev block of the Kuznetsk-Alatau (Table 1; Fig. 3) were analysed. Samples TV-78 and 79 come from the granite–(grano)diorite Beloiyus massif. TV-82 was collected from a dolerite dyke from the island-arc (monzo)diorite–gabbroid sequence (late stage island-arc magmatism). TV-84 and TV-85 originate from the (grano)dioritic Tuim-Karish massif. These (grano)diorites and their Cambrian host rocks are cut by a Middle Devonian erosion surface containing (grano)dioritic clasts (Fig. 3b). This shows that the massif was exhumed at this time. A contact aureole of the Tuim-Karish massif is expressed in the Cambrian limestones, which are metamorphosed to marbles and diopside-, garnet- and/or magnetite-bearings skarns (Fig. 3b).

Zircon U/Pb (ZUPb) dating (TV-82, TV-85) was performed using Laser Ablation-Inductively Coupled Plasma-Mass Spectrometry (LA-ICP-MS) following the procedures discussed by Glorie *et al.* (2010).

Titanite fission-track (TFT) dating was performed, and spontaneous tracks were etched with 0.4% HF (24 h, 20 °C) induced tracks in a muscovite external detector (ED) with 40% HF (40 min, 20 °C). Apatite fission-track (AFT) dating procedures are described in De Grave *et al.* (2008). Spontaneous tracks were etched with 2.5% HNO_3 (70 s, 25 °C) (induced tracks as for TFT). A total of 100 horizontal confined tracks were measured to construct an AFT length–frequency distribution, and thermal history modelling was performed using HeFTy software (Ketcham, 2005). Irradiations for AFT and TFT were done at the BR1 facility (Belgian Nuclear Research Centre). Apatite (U–Th–Sm)/He (AHe) analysis was carried out at Kansas State University (USA) with procedures described by Blackburn *et al.* (2008).

Results and discussion

The TV-82 dolerite dyke yields a concordant ZUPb age of 496 ± 7 Ma (Late Cambrian), and the TV-85 granodiorite of the Tuim-Karish massif gives a concordant age of 477 ± 5 Ma (Early Ordovician) (Table 2, Fig. 4). The age of 496 ± 7 Ma for TV-82 constrains the latest stages of island-arc magmatism to the Paibian, Late Cambrian. The initial stages of the island-arc are dated to the Late Ediacaran–Early Cambrian, reaching a mature stage in the Middle Cambrian (Kazansky *et al.*, 2003). Earlier reports by e.g. Rudnev *et al.* (2004, 2008) gave ZUPb ages of *c.* 470–500 Ma for collisional granitoids in Kuznetsk-Alatau, and Vladimirov *et al.* (2001) cite *c.* 469–492 Ma. $^{40}Ar/^{39}Ar$ amphibole dating on the igneous rocks in the region yields plateau ages of *c.* 477–481 Ma (Sotnikov *et al.*, 2001). The Early-Ordovician emplacement age of the Tuim-Karish granodiorite (TV-85) at 477 ± 5 Ma is contemporaneous with this age of collision of the island-arc with Siberia. Several other studies indicate that the Kuznetsk-Alatau island-arc (as part of a larger 'Altai' island-arc system) accreted to Siberia in the Early Ordovician (Buslov *et al.*, 2002; Kazansky *et al.*, 2003; Dobretsov and Buslov, 2007; Buslov, 2011). The Tuim-Karish and other granitoids of the Iuys-Batenev block were exhumed by the Early Devonian as attested by an erosional contact between the Cambrian and Early Devonian rocks. We mapped this contact in the Matarak-Itkul lake region (Fig. 3).

The TFT age for diorite TV-78 from the Beloiyus massif is 226 ± 11 Ma (Table 3; Fig. 3). TFT ages are cooling ages as titanite cools through the TFT partial annealing zone (PAZ) of ~265–310 °C (Coyle and Wagner, 1998). The obtained TFT age there-

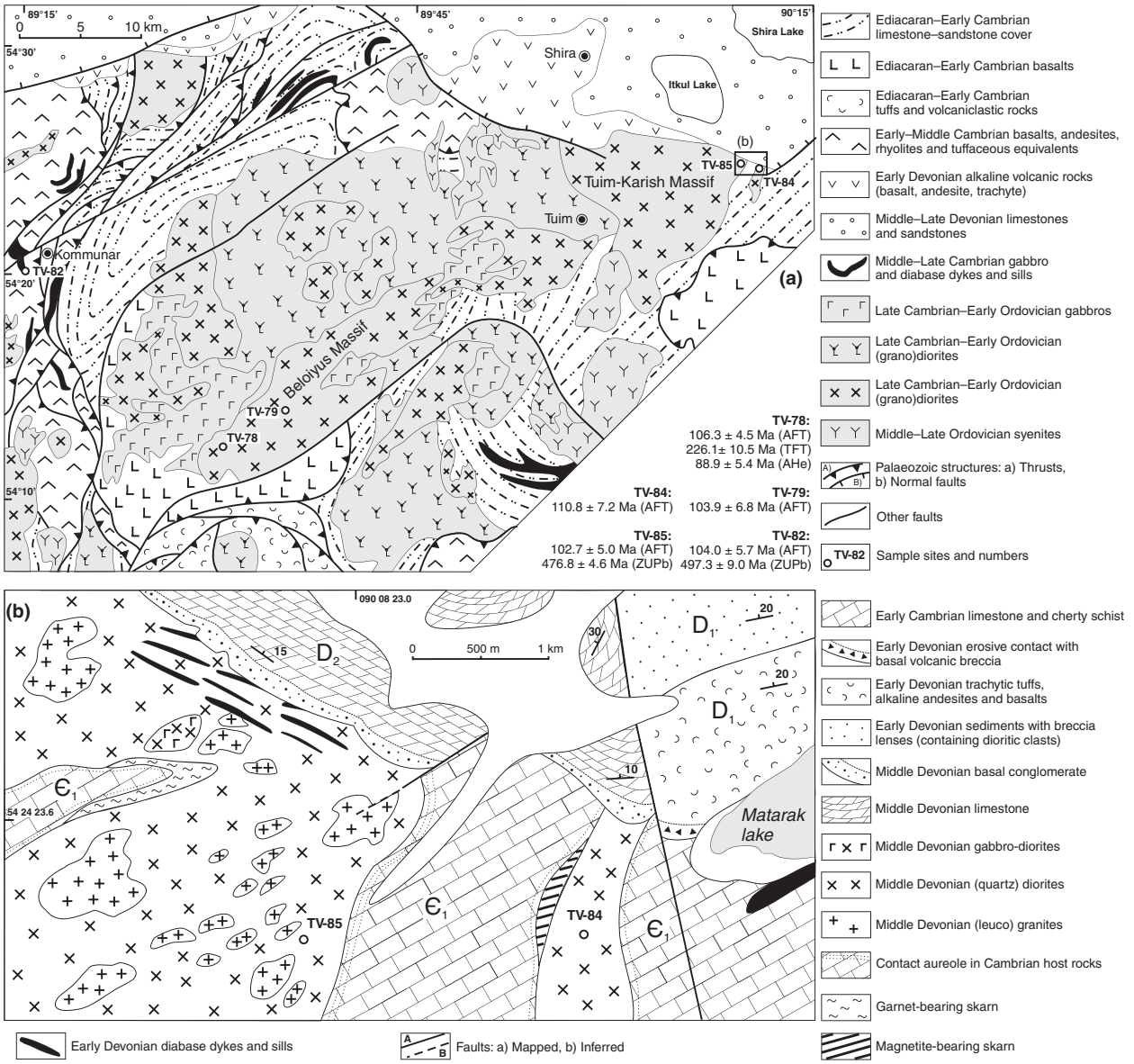

Fig. 3 (a) Geological sketch map of the Iuys-Batenev study area of the Kuznetsk-Alatau terrane with its island-arc basement and intrusive massifs (modified after Krasilnikov *et al.*, 1959; Sekretarev and Lipishanov, 2000). (b) Detailed map of the northern contact zone between the Tuim-Karish massif and the Devonian deposits of the North Minusa Basin.

fore represents a Late Triassic (Ladinian–Carnian, Middle–Late Triassic transition) basement cooling that affected the Kuznetsk-Alatau. The most reasonable interpretation is that the basement cooling transpired through denudation and exhumation near the Middle–Late Triassic boundary. The sediments in all adjoining basins (Kuznetsk, Minusa, southeastern West Siberian Basin) indicate a hiatus and angular unconformity between the Permian–Middle Triassic and Jurassic (Le Heron *et al.*, 2008; Davies *et al.*, 2010), supporting this hypothesis. Moreover, sediments below the unconformity show signs of compressional deformation. These observations point to an important Late Triassic–Early Jurassic orogenic event. The denudation of the Kuznetsk-Alatau can be related to an early phase of construction of the Mongol–Okhotsk Orogen (Fig. 1) due to clockwise rotation of Siberia (Kravchinsky *et al.*, 2002; Cogné *et al.*, 2005; Metelkin *et al.*, 2010). This denudation could have been enhanced by a base-level drop related to rifting in the West Siberian Basin (Aplonov, 1995; Allen *et al.*, 2006; Vyssotski *et al.*, 2006).

Considering the analytical uncertainty of 11 Ma on the TFT age, the cooling post-dates the main Siberian Flood Basalt event (Permian–Triassic boundary) by at least 10–25 Ma. These flood basalts are associated with the Siberian mega-mantle-plume that is linked to perturbation of the mantle convection systems during transition from Pangaea assembly to break-up (Nikishin *et al.*, 2002; Reichow *et al.*, 2009). This event might have heated

Table 1 Sample details and applied methods.

Sample	Latitude	Longitude	Altitude (m)	Locality	Lithology	Method
TV-78	N54°11′50″	E089°30′48″	595	Mendol	Diorite	AFT, AHe, TFT
TV-79	N54°13′47″	E089°34′47″	590	Mendol	Granite	AFT
TV-82	N54°20′08″	E089°15′42″	775	Kommunar	Dolerite	AFT, ZUPb
TV-84	N54°23′52″	E090°09′52″	630	Shira, Tuim	Granodiorite	AFT
TV-85	N54°23′54″	E090°07′50″	530	Shira, Tuim	Granodiorite	AFT, ZUPb

AFT, Apatite fisson-track (method); AHe, Apatite (U–Th–Sm)/He; ZUPb, Zircon U/Pb.

the Kuznetsk-Alatau basement after which it would have cooled down through the TFT PAZ. However, considering the time lag of at least 10–25 Ma, the distance to the Siberian Traps and the fact that basement heating must have exceeded ~265–310 °C, it seems unlikely that this process is directly linked to the 226 ± 11 Ma TFT age for the Beloiyus diorite. It might have contributed to a lesser amount, but it seems more reasonable to explain the cooling by denudation.

Apatite fission-track ages for all samples range between *c.* 103 and 111 Ma (Albian, Early Cretaceous) (Table 3; Fig. 3), and mean track lengths between ~12.5 and 13.2 μm (Fig. 5). Using the TFT age and an average AHe age of 89 ± 5 Ma for sample TV-78 as constraints, apatite data were used for thermal history modelling (HeFTy software, Ketcham, 2005; Ketcham *et al.*, 2007) (Fig. 5). The resulting models consistently indicate Late Jurassic–Early Cretaceous cooling, implying significant denudation–exhumation of the Altai–Sayan and Kuznetsk-Alatau at that time. Hence, this event is responsible for important Jurassic–Cretaceous sediment supply to the West Siberian, Kuznetsk and Minusa Basin (Le Heron *et al.*, 2008; Davies *et al.*, 2010). Rifting in the West Siberian Basin increased the accommodation space for the sediments (Aplonov, 1995; Allen *et al.*, 2006; Vyssotski *et al.*, 2006).

Apatite fission-track and thermal history data from regions adjacent to the Kuznetsk-Alatau, such as in the Siberian Altai–Sayan (De Grave and Van den haute, 2002; De Grave *et al.*,

Table 2 Zircon LA-ICP-MS U/Pb dating results for samples TV-82 (Kommunar) and TV-85 (Tuim-Karish).

No	^{207}Pb* (cps)	U† (ppm)	Pb† (ppm)	Th†/U	^{206}Pb/^{204}Pb	^{206}Pb‡/^{238}U	±2σ (%)	^{207}Pb‡/^{235}U	±2σ (%)	^{207}Pb‡/^{206}Pb	±2σ (%)	Rho§	^{206}Pb¶/^{238}U	±2σ (Ma)	^{207}Pb¶/^{235}U	±2σ (Ma)	Concordia††
TV-82																	
1	9154	793	73	0.90	2564	0.0756	6.3	0.5827	7.4	0.0559	3.8	0.86	470	29	466	28	99
2	7832	631	63	0.96	4879	0.0800	4.1	0.6383	7.6	0.0579	6.3	0.55	496	20	501	30	101
3	7325	624	63	1.08	7265	0.0787	3.8	0.6091	5.6	0.0561	4.1	0.68	489	18	483	22	99
4	3212	264	24	0.63	3265	0.0790	4.7	0.6226	7.3	0.0572	5.6	0.65	490	22	491	29	100
5	6841	556	53	0.87	6209	0.0795	4.2	0.6324	5.9	0.0577	4.1	0.71	493	20	498	23	101
6	7718	615	57	0.65	4867	0.0825	4.1	0.6676	6.6	0.0587	5.2	0.62	511	20	519	27	102
7	1751	140	12	0.48	2416	0.0820	5.5	0.6916	7.8	0.0612	5.4	0.71	508	27	534	33	105
8	8888	731	77	1.25	7184	0.0805	3.4	0.6931	8.4	0.0624	7.6	0.41	499	17	535	35	107
9	4073	342	29	0.45	1435	0.0805	4.7	0.6678	7.8	0.0602	6.2	0.61	499	23	519	32	104
TV-85																	
1	1063	98	8	0.62	427	0.0746	3.2	0.5832	7.4	0.0567	6.7	0.43	464	14	467	28	101
2	911	80	7	0.62	738	0.0761	3.0	0.6298	9.7	0.0600	9.2	0.31	473	14	496	39	105
3	1055	89	8	0.57	785	0.0800	3.8	0.6665	13.1	0.0604	12.5	0.29	496	18	519	54	105
4	735	60	5	0.52	1019	0.0764	4.4	0.7030	10.7	0.0667	9.7	0.41	475	20	541	46	114
5	908	83	7	0.47	980	0.0754	3.3	0.6128	6.8	0.0590	5.9	0.49	469	15	485	26	104
6	892	84	7	0.43	956	0.0792	4.5	0.5999	8.7	0.0549	7.5	0.51	492	21	477	34	97
7	699	64	5	0.55	628	0.0780	5.3	0.6480	9.5	0.0602	7.9	0.56	484	25	507	39	105
8	1118	113	9	0.64	741	0.0749	3.1	0.5686	8.1	0.0551	7.5	0.38	465	14	457	30	98
9	2405	226	18	0.30	2186	0.0771	4.0	0.5832	6.5	0.0549	5.1	0.62	479	19	466	25	97
10	897	82	7	0.61	3041	0.0759	3.8	0.6181	9.5	0.0591	8.7	0.41	472	18	489	38	104
11	1164	110	9	0.59	930	0.0785	3.8	0.6150	7.5	0.0568	6.4	0.51	487	18	487	29	100
12	865	82	6	0.38	790	0.0772	3.7	0.6243	9.6	0.0587	8.8	0.38	479	17	493	38	103
13	1392	133	11	0.54	924	0.0786	3.9	0.6224	8.6	0.0575	7.7	0.45	488	18	491	34	101
14	1486	141	12	0.63	1286	0.0772	3.6	0.6223	6.5	0.0585	5.4	0.55	479	17	491	26	102
TV-82	**6310**	**522**	**50**	**0.81**	**4454**	**0.0798**	**4.6**	**0.6450**	**7.1**	**0.0586**	**5.4**	**0.64**	**495**	**22**	**505**	**29**	**102**
TV-85	**1114**	**103**	**9**	**0.53**	**1102**	**0.0771**	**3.8**	**0.6212**	**8.7**	**0.0585**	**7.8**	**0.45**	**479**	**18**	**490**	**35**	**102**

*Within-run, background-corrected mean ^{207}Pb signal.

†U and Pb content and Th/U ratio were calculated relative to the GJ-1 zircon standard.

‡Corrected for: background, within-run Pb/U fractionation (^{206}Pb/^{238}U), where needed common Pb (Stacey and Kramers, 1975) and subsequently normalized to GJ-1 (instrumental drift corrected).

§Rho is the error correlation defined as err^{206}Pb/^{238}U / err^{207}Pb/^{235}U.

¶U/Pb ages were calculated with Isoplot (Ludwig, 2003).

††Degree of concordance = age^{206}Pb/^{238}U/age^{207}Pb/^{206}Pb × 100.

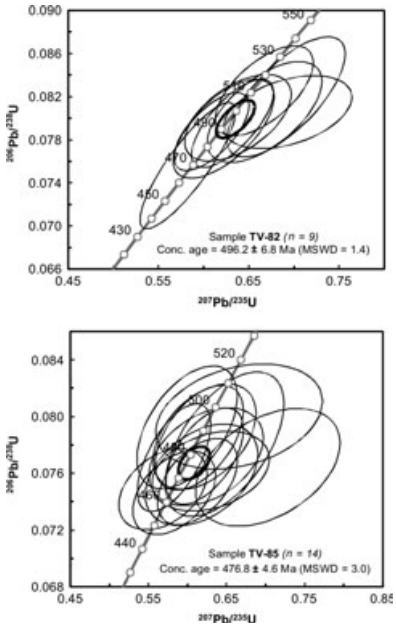

Fig. 4 Zircon U/Pb Concordia plots for samples TV-82 (Kommunar) and TV-85 (Tuim-Karish) (both concordant ages).

2008, 2009), East Sayan–Baikal (Van der Beek *et al.*, 1996; Jolivet *et al.*, 2009), the Chinese Altai (Yuan *et al.*, 2006) and Western Mongolia (Jolivet *et al.*, 2007; Vassallo *et al.*, 2007), in general, show similar observations.

The Late Jurassic–Early Cretaceous denudation–exhumation of Kuznetsk-Alatau and Altai–Sayan is coeval with the main phase of the Mongol–Okhotsk orogeny (Fig. 6) and diachronous closure of the Mongol–Okhotsk Ocean between Siberia and North China–Mongolia (Amur or Sino-Korean continent). Initial stages transpired in the Triassic in the western sections near the Altai–Sayan and Transbaikal area, whereas the main Jurassic–Cretaceous phase occurred more to the east as a consequence of scissors-like closure of the basin (Zorin, 1999; Kravchinsky *et al.*, 2002; Cogné *et al.*, 2005; Metelkin *et al.*, 2010). Although clearly a strong relief was created in our study area at that time (Le Heron *et al.*, 2008; Davies *et al.*, 2010), it is still a matter of controversy to which extent it is related to the Mongol–Okhotsk closure. Similar Jurassic–Cretaceous AFT ages are found throughout the southern sections of the CAOB, most notably in the Tien Shan orogen. Mesozoic reactivation of the Tien Shan is often related to the Cimmerian orogeny and collision of the Qiangtang and Lhasa blocks to Eurasia (Dumitru *et al.*, 2001; Glorie *et al.*, 2010; Jolivet *et al.*, 2010). In any case, it is clear that during the Mesozoic the entire CAOB was subjected to large scale reactivation as far-field effects of collision–accretion events shaping the Asian continent.

Conclusions

1 The latest magmatic stages of the Ediacaran–Cambrian Kuznetsk-Alatau island-arc (dolerite dykes) are dated to the Late Cambrian (*c.* 496 Ma).
2 Collision of the Kuznetsk-Alatau island-arc with Siberia occurred in the Early Ordovician. Emplacement of the collisional Tuim-Karish granodiorite in our study area was dated to *c.* 477 Ma.
3 An Early Devonian erosional surface reveals that the Tuim-Karish massif had been exhumed by that time.

Table 3 Thermochronology results.

AFT

Sample	*n*	ρ_s (±1σ)	N_s	ρ_i (±1σ)	N_i	ρ_d (±1σ)	N_d	ρ_s/ρ_i	$P(\chi^2)$	Age$_\zeta$ (Ma)	l_m(μm)	n_l	σ(μm)
TV-78	20	3.225 (0.068)	2263	1.588 (0.048)	1109	4.122 (0.080)	2637	2.054 ± 0.075	0.99	106.3 ± 4.5	13.2	100	1.4
TV-79	20	0.926 (0.033)	782	0.481 (0.024)	400	4.144 (0.080)	2651	1.998 ± 0.123	0.99	103.9 ± 6.8	–	–	–
TV-82	20	1.475 (0.043)	1162	0.749 (0.031)	589	4.167 (0.081)	2666	1.989 ± 0.101	0.99	104.0 ± 5.7	13.0	100	1.5
TV-84	20	1.083 (0.037)	837	0.516 (0.026)	394	4.161 (0.081)	2662	2.122 ± 0.130	1.00	110.8 ± 7.2	12.5	100	1.9
TV-85	20	5.156 (0.127)	1650	2.459 (0.088)	787	3.692 (0.076)	2386	2.216 ± 0.096	0.75	102.7 ± 5.0	13.2	100	1.8

TFT

Sample	*n*	ρ_s (±1σ)	N_s	ρ_i (±1σ)	N_i	ρ_d (±1σ)	N_d	ρ_s/ρ_i	$P(\chi^2)$	Age$_\zeta$ (Ma)
TV-78	23	5.764 (0.125)	2121	2.603 (0.084)	958	4.048 (0.080)	2591	2.251 ± 0.088	0.90	226.1 ± 10.5

AHe

Sample	Aqt	U (ppm)	Th (ppm)	Sm (ppm)	Th/U	He (nmol μg^{-1})	m (μg)	F_T	Age (Ma)	Average	σ (t_m) (Ma)
TV-78	1	6.7	17.6	47.7	2.6	4.37	4.9	0.72	99.5 ± 4.5		
	2	**5.1**	**16.1**	**26.5**	**3.2**	**2.84**	**5.4**	**0.74**	**78.3 ± 4.7**		
	3	14.0	37.5	62.1	2.7	9.00	2.9	0.68	104.2 ± 6.3	88.9 ± 5.4	15.0

AFT, apatite fission-track dating, TFT, titanite fission-track dating, AHe, apatite (U–Th–Sm)/He dating. AFT age and length data; TFT age data: *n* is the number of counted grains; ρ_s, ρ_i and ρ_d are the density of spontaneous, induced tracks and induced tracks in an external detector (ED) irradiated against a dosimeter glass. The ρ_d-values are interpolated values from regularly spaced glass dosimeters (IRMM-540). ρ_d is expressed as 10^5 tracks per cm^2; ρ_s and ρ_i as 10^6 tracks per cm^2. N_s, N_i and N_d (interpolated) are the number of counted spontaneous, induced tracks and induced tracks in the ED. $P(\chi^2)$ is the Chi-squared probability that the dated grains have a constant ρ_s/ρ_i-ratio. A calibration factor or ζ-value of 253.1 ± 2.4 a.cm^2 (AFT) and 505.1 ± 7.8 a.cm^2 (TFT) was used for age calculation based on Mount Dromedary and Fish Canyon Tuff titanite, and Durango and Fish Canyon Tuff apatite age standards and the IRMM-540 glass. AFT length data: mean track length (l_m) with standard deviation σ, obtained from the measurement of a number (n_l) of natural, horizontal confined tracks. AHe dating results: Aqt, Aliquot number. Concentrations for U, Th and Sm are listed in ppm, the ^{4}He concentration in nmol μg^{-1}; m, mass of the apatite grains. F_T is the α-ejection correction factor (Farley, 2002). Single grain ages for each aliquot are given, and an average sample value is calculated. Aliquot 2 (in bold) gives a somewhat younger age with respect to both other analyses, but there seems no immediate reason to reject it.

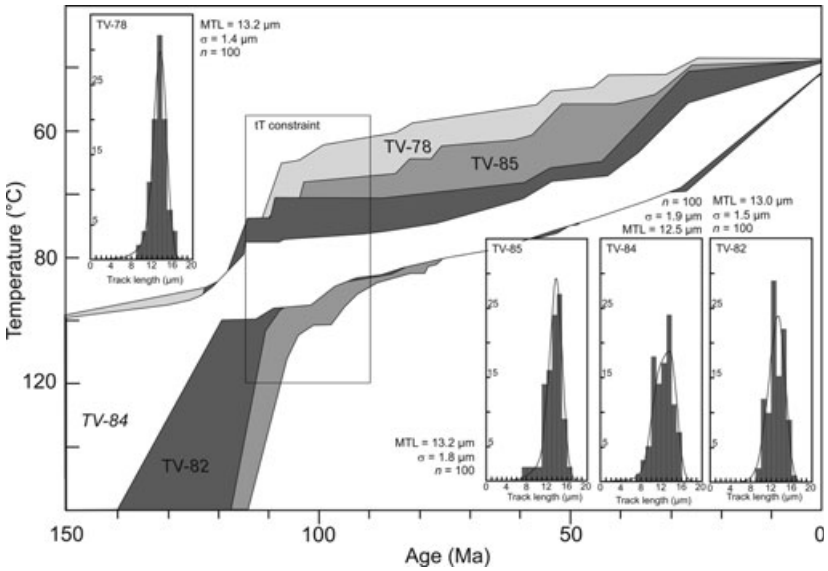

Fig. 5 Modelled thermal histories obtained from AFT input (and AHe for sample TV-78), using HeFTy software (Ketcham, 2005) and Ketcham *et al.* (2007) annealing equations. Only 'good-fit' (Ketcham, 2005) envelopes are shown. Track length distributions are indicated for the four modelled samples (TV-79 did not yield enough confined tracks): MTL, mean track length, **σ**, standard deviation of MTL, n = number of horizontal confined tracks measured (no ^{252}Cf or heavy ion-irradiation was applied, no c-axis projection was applied). The TFT age of 226 ± 11 Ma, at TFT PAZ temperatures of 265–310 °C (Coyle and Wagner, 1998) was inserted as tT box constraint for high-temperature benchmark. An additional constraint at AFT ages and AFT PAZ temperatures was used for inverse modelling. The Monte-Carlo search method was utilized and 50 000–150 000 paths were calculated.

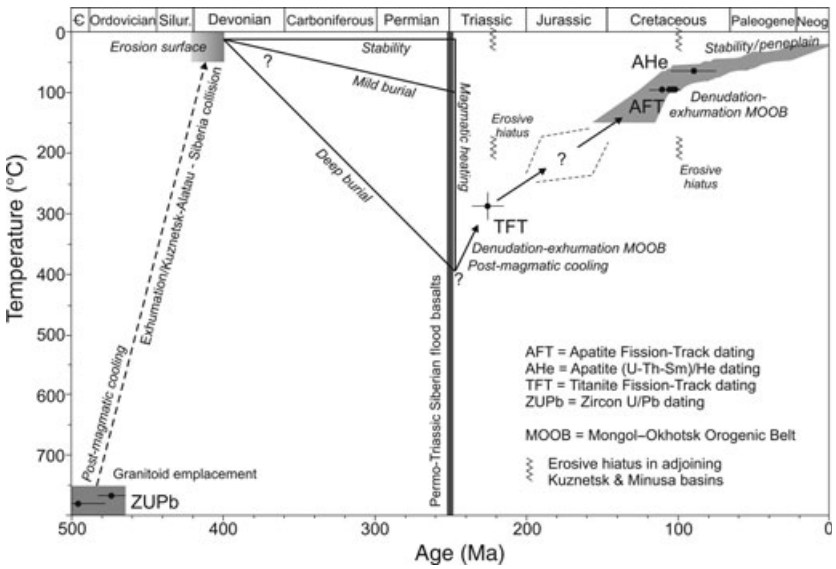

Fig. 6 General thermo-tectonic model for Kuznetsk-Alatau. After emplacement (Late Cambrian–Early Ordovician), the granitoid basement reached surface temperatures due to post-magmatic cooling and rapid exhumation as a result of collision with Siberia. By the Early Devonian, an erosive surface developed on the granitoids and their host rocks. Although magmatic heating of the basement as a consequence of the Siberian mega-plume and associated Permo-Triassic flood basalts cannot be ruled out, it is most probably re-burial underneath Devonian–Middle Triassic sediments (as in the adjoining Kuznetsk and Minusa basins) that re-heated the granitoids past TFT 'closure' temperatures (resetting the TFT system). The Middle–Late Triassic TFT cooling age of the basement corresponds to a sedimentary hiatus in the adjoining basins and points to an orogenically driven exhumation event. This exhumation might have been continuous up to the Early–Late Cretaceous transition as indicated by AFT and AHe thermochronology. By the Late Cretaceous, the Kuznetsk-Alatau basement was cooled to shallow crustal temperatures as a peneplanation surface developed. Slow denudation–exhumation through the Cenozoic eventually cooled the granitoids and brought them to their present outcrop position.

4 A TFT age of *c*. 226 Ma points to denudation/exhumation of the basement at the Middle–Late Triassic transition. This is possibly related to initial closure of the Mongol–Okhotsk Ocean and rifting in the West Siberian Basin. Post-magmatic cooling succeeding the Siberian mega-plume events might have had a secondary influence.
5 Early Cretaceous AFT ages and thermal history modelling reveal Late Jurassic–Early Cretaceous cooling of the Kuznetsk-Alatau basement. This might be linked to denudation in the context of the Mongol–Okhotsk orogeny. This produced important sedimentary influx into the Kuznetsk, Minusa and West Siberian Basins that are of large economic significance.
6 The Mesozoic is an era of large-scale reactivation of the entire CAOB, from the northern sections, as demonstrated here, to the south (e.g. Tien Shan).

Acknowledgements

JDG is supported by FWO – Flanders, SG by IWT – Flanders. We are indebted to Drs Vittiglio and Vermaercke for help with irradiations at the Belgian Nuclear Research Centre. We are grateful to Dr Stockli, Kansas State University for AHe analyses and B. Jourquin for sample preparation assistance. This research was co-funded by Ghent University (BOF –project 01SB1309) and the SB-RAS (Integration Project, N21). This paper benefitted from insightful reviews by Marc Jolivet and Mark Allen.

References

Allen, M.B. and Davies, C.E., 2007. Unstable Asia: active deformation of Siberia revealed by drainage shifts. *Basin Res*., **19**, 379–392.

Allen, M.B., Anderson, L., Searle, R.C. and Buslov, M., 2006. Oblique rift geometry of the West Siberian Basin: tectonic setting for the Siberian flood basalts. *J. Geol. Soc. London*, **163**, 901–904.

Aplonov, S.V., 1995. The tectonic evolution of West Siberia: an attempt at a geophysical analysis. *Tectonophysics*, **245**, 61–84.

Blackburn, T.J., Stockli, D.F., Carlson, R.W. and Berendsen, P., 2008. (U–Th)/He dating of kimberlites – a case study from north-eastern Kansas. *Earth Planet. Sci. Lett*., **275**, 111–120.

Buslov, M.M., 2011. Tectonics and geodynamics of Central Asian Foldbelt: the role of Late Paleozoic large-amplitude displacements. *Russian Geol. Geophys*., **52**, 7–26.

Buslov, M.M., Watanabe, T., Saphonova, I.Y., Iwata, K., Travin, A. and Akiyama, M., 2002. A Vendian-Cambrian Island Arc system of the Siberian continent in Gorny Altai (Russia, Central Asia). *Gondwana Res*., **5**, 781–800.

Buslov, M.M., Watanabe, T., Smirnova, L.V., Fujiwara, I., Iwata, K., De Grave, J., Semakov, N.N., Travin, A.V., Kiryanova, A.P. and Kokh, D.A., 2003. Role of strike-slip faults in Late Paleozoic-Early Mesozoic tectonics and geodynamics of the Altai-Sayan and East Kazakhstan folded zone. *Russian Geol. Geophys*., **44**, 49–75.

Buslov, M.M., Safonova, I.Y., Fedoseev, G.S., Reichow, M.K., Davies, C.E. and Babin, G.A., 2010. Permo-Triassic plume magmatism of the Kuznetsk Basin, Central Asia: geology, geochronology, and geochemistry. *Russian Geol. Geophys*., **51**, 1021–1036.

Cogné, J.P., Kravchinsky, V.A., Halim, N. and Hankard, F., 2005. Late Jurassic-Early Cretaceous closure of the Mongol-Okhotsk Ocean demonstrated by new Mesozoic paleomagnetic results from the Trans-Baikal area (SE Siberia). *Geophys. J. Int*., **163**, 813–832.

Coyle, D.A. and Wagner, G.A., 1998. Positioning the titanite fission-track partial annealing zone. *Chem. Geol*., **149**, 117–125.

Davies, C., Allen, M.B., Buslov, M.M. and Safonova, I., 2010. Deposition in the Kuznetsk Basin, Siberia: insights into Permian-Triassic transition and the Mesozoic evolution of Central Asia. *Palaeogeogr. Palaeoclimatol. Palaeoecol*., **295**, 307–322.

De Grave, J. and Van den haute, P., 2002. Denudation and cooling of the Lake Teletskoye region in the Altai Mountains (South Siberia) as revealed by apatite fission-track thermochronology. *Tectonophysics*, **349**, 145–159.

De Grave, J., Buslov, M.M. and Van den haute, P., 2007. Distant effects of India-Eurasia convergence and Mesozoic intracontinental deformation in Central Asia: constraints from apatite fission-track thermochronology. *J. Asian Earth Sci*., **29**, 188–204.

De Grave, J., Van den haute, P., Buslov, M.M., Dehandschutter, B. and Glorie, S., 2008. Apatite fission-track thermochronology applied to the Chulyshman Plateau, Siberian Altai Region. *Radiat. Meas*., **43**, 38–42.

De Grave, J., Buslov, M.M., Van den haute, P., Metcalf, J., Dehandschutter, B. and Mc Williams, M.O., 2009. Multi-Method chronometry of the Teletskoye graben and its basement, Siberian Altai Mountains: new insights on its thermotectonic evolution. *Geol. Soc. London Spec. Publ*., **324**, 237–259.

Dobretsov, N.L. and Buslov, M.M., 2007. Late Cambrian–Ordovician tectonics and geodynamics of Central Asia. *Russian Geol. Geophys*., **48**, 71–82.

Dumitru, T.A., Zhou, D., Chang, E.Z. and Graham, S.A., 2001. Uplift, exhumation, and deformation in the Chinese Tian Shan. *Geol. Soc. Am. Mem*., **194**, 71–99.

Farley, K.A., 2002. (U-Th)/He dating: techniques, calibrations, and applications. *Rev. Mineral. Geochem*., **47**, 819–844.

Fedoseev, G.S., 2008. The role of mafic magmatism in age specification of Devonian continental trough deposits: evidence from the Minusa Basin, western Siberia, Russia. *Bull. Geosci*., **83**, 473–480.

Glorie, S., De Grave, J., Buslov, M.M., Elburg, M.A., Stockli, D.F., Van den haute, P. and Gerdes, A., 2010. Multi-method chronometric constraints on the evolution of the Northern Kyrgyz Tien Shan batholith: from emplacement to exhumation. *J. Asian Earth Sci*., **38**, 131–146.

Jolivet, M., Ritz, J.-F., Vassallo, R., Larroque, C., Braucher, R., Todbileg, M., Chauvet, A., Sue, C., Arnaud, N., De Vicente, R., Arzhanikova, A. and Arzhanikov, S., 2007. Mongolian summits: an uplifted, flat, old but still preserved erosion surface. *Geology*, **35**, 871–874.

Jolivet, M., De Boisgrollier, T., Petit, C., Fournier, M., Sankov, V.A., Ringenbach, J.-C., Byzov, L., Miroshnichenko, A.I., Kovalenko, S.N. and Anisimova, S.V., 2009. How old is the Baikal Rift Zone? Insights from apatite fission track thermochronology. *Tectonics*, **28**, TC3008, doi: 10.1029/2008TC002404.

Jolivet, M., Dominguez, S., Charreau, J., Chen, Y., Li, Y. and Wang, Q., 2010. Mesozoic and Cenozoic tectonic history of the central Chinese Tian Shan: reactivated tectonic structures and active deformation. *Tectonics*, **29**, TC6019, doi: 10.1029/2010TC002712.

Kazansky, A.Y., Metelkin, D.V., Kungurtsev, L.V. and Kizub, P.A., 2003. Kinematics of the Martaiga block of the Kuznetsk-Alatau paleoisland arc during the Late Vendian–Early Ordovician as inferred from paleomagnetic data. *Russian Geol. Geophys*., **44**, 187–201.

Ketcham, R.A., 2005. Forward and inverse modeling of low-temperature thermochronometry data. *Rev. Mineral. Geochem*., **58**, 275–314.

Ketcham, R.A., Carter, A., Donelick, R.A., Barbarand, J. and Hurford, A.J.,

2007. Improved modelling of fission-track annealing in apatite. *Am. Mineral.*, **92**, 799–810.

Khain, E.V., Bibikova, E.V., Salnikova, E.B., Kröner, A., Gibsher, A.S., Didenko, A.N., Degtyarev, K.E. and Fedotova, A.A., 2003. The Palaeo-Asian Ocean in the Neoproterozoic and early Palaeozoic: new geochronologic data and palaeotectonic reconstructions. *Precambrian Res.*, **122**, 329–358.

Krasilnikov, B.N., Verzhkhovskaya, V.A. and Kryazheva, L.V., 1959. Geological map of the USSR, 1: 200,000, Minusa Series sheet N-46-XIII, VSEGEI, Leningrad.

Kravchinsky, V.A., Cogné, J.-P., Harbert, W.P. and Kuzmin, M.I., 2002. Evolution of the Mongol-Okhotsk ocean as constrained by new paleomagnetic data from the Mongol-Okhotsk suture zone, Siberia. *Geophys. J. Int.*, **148**, 34–57.

Le Heron, D.P., Buslov, M.M., Davies, C., Richards, K. and Safonova, I., 2008. Evolution of Mesozoic fluvial systems along the SE flank of the West Siberian Basin, Russia. *Sed. Geol.*, **208**, 45–60.

Ludwig, K., 2003. *User's Manual for Isoplot 3.00, A Geochronological Toolkit for Microsoft Excel v. 4*. Berkeley Geochronology Center Special Publication Available online at: http://www.bgc.org/isoplot_etc/Isoplot3betaManual.pdf.

Metelkin, D.V., Vernikovsky, V.A., Kazansky, A.Y. and Wingate, M.T.D., 2010. Late Mesozoic tectonics of Central Asia based on paleomagnetic evidence. *Gondwana Res.*, **18**, 400–419.

Nikishin, A.M., Ziegler, P.A., Abbott, D., Brunet, M.-F. and Cloetingh, S., 2002. Permo-Triassic intraplate magmatism and rifting in Eurasia: implications for mantle plumes and mantle dynamics. *Tectonophysics*, **351**, 3–39.

Novikov, I.S., Sokol, E.V., Travin, A.V. and Novikova, S.A., 2008. Signature of Cenozoic orogenic movements in combustion metamorphic rocks: mineralogy and geochronology (example of the Salair-Kuznetsk basin transition). *Russian Geol. Geophys.*, **49**, 378–396.

Reichow, M.K., Pringle, M.S., Al'Mukhamedov, A.I., Allen, M.B., Andreichev, V.L., Buslov, M.M., Davies, C.E., Fedoseev, G.S., Fitton, J.G., Inger, S., Medvedev, A.Y., Mitchell, C., Puchkov, V.N., Safonova, I.Y., Scott, R.A. and Saunders, A.D., 2009. The timing and extent of the eruption of the Siberian Traps large igneous province: implications for the end-Permian environmental crisis. *Earth Planet. Sci. Lett.*, **277**, 9–20.

Rudnev, S.N., Vladimirov, A.G., Ponomarchuk, V.A., Kruk, N.N., Babin, G.A. and Borisov, S.M., 2004. Early Palaeozoic granitoid batholiths of the Altai-Sayan folded region (lateral-temporal zoning and sources). *Doklady Earth Sci.*, **396**, 492–495 [in Russian].

Rudnev, S.N., Borisov, S.M., Babin, G.A., Levchenkov, O.A., Makeev, A.F., Serov, P.A., Matukov, D.I. and Plotkina, Y.V., 2008. Early Paleozoic batholiths in the Northern Part of the Kuznetsk Alatau: composition, age and sources. *Petrology*, **16**, 395–419.

Sekretarev, M.N. and Lipishanov, A.P., 2000. Geological map of the Russian Federation, scale 1/200,000, Minusa Series, sheet N-45-XVIII, VSEGEI, Saint-Petersburg (In Russian).

Şengör, A.M.C., Natal'in, B.A. and Burtman, V.S., 1993. Evolution of the Altaid tectonic collage and Palaeozoic crustal growth in Eurasia. *Nature*, **364**, 299–307.

Sotnikov, V.I., Ponomarchuk, V.A., Shevchenko, D.O., Berzina, A.P. and Berzina, A.N., 2001. $^{40}Ar/^{39}Ar$ geochronology of magmatic and metasomatic events in the Sora porphyry Cu-Mo ore cluster (Kuznetsk Alatau). *Russian Geol. Geophys.*, **42**, 744–758.

Stacey, J.S. and Kramers, J.D., 1975. Approximation of terrestrial lead isotope evolution by a two–stage model. *Earth Planet. Sci. Lett.*, **26**, 207–221.

Van der Beek, P., Delvaux, D., Andriessen, P.A.M. and Levi, K.G., 1996. Early Cretaceous denudation related to convergent tectonics in the Baikal region, SE Siberia. *J. Geol. Soc. London*, **153**, 515–523.

Vassallo, R., Jolivet, M., Ritz, J.-F., Brauchner, R., Larroque, C., Sue, C., Todbileg, M. and Javkhlanbold, D., 2007. Uplift age and rates of the Gurvan Bogd system (Gobi-Altay) by apatite fission track analysis. *Earth Planet. Sci. Lett.*, **259**, 333–346.

Vladimirov, A.G., Kozlov, M.S., Shokalskii, S.P., Khalilov, V.A., Rudnev, S.N., Kruk, N.N., Vystavnoi, S.A., Borisov, S.M., Berezikov, Y.K., Metsner, A.N., Babin, G.A., Mamlin, A.N., Murzin, O.M., Nazarov, G.V. and Makarov, V.A., 2001. Major epochs of intrusive magmatism of Kuznetsk Alatau, Altai, and Kalba (from U-Pb isotope dates). *Russian Geol. Geophys.*, **42**, 1089–1109.

Vyssotski, A.V., Vyssotski, V.N. and Nezhdanov, A.A., 2006. Evolution of the West Siberian Basin. *Mar. Petrol. Geol.*, **23**, 93–126.

Windley, B.F., Alexeiev, D., Xiao, W., Kröner, A. and Badarch, G., 2007. Tectonic models for accretion of the Central Asian Orogenic Belt. *J. Geol. Soc. London*, **164**, 31–47.

Yuan, W.-M., Carter, A., Dong, J.-Q., Bao, Z., An, Y. and Guo, Z., 2006. Mesozoic-Tertiary exhumation history of the Altai Mountains, northern Xinjiang, China: new constraints from apatite fission track data. *Tectonophysics*, **412**, 183–193.

Zorin, Y.A., 1999. Geodynamics of the western part of the Mongolia-Okhotsk collisional belt, Trans-Baikal region (Russia) and Mongolia. *Tectonophysics*, **306**, 33–56.

Received 06 December 2010; revised version 10 March 2011; accepted 30 April 2011

